Molecular Dynamics Simulations of Ground and Transition States for the S_N2 Displacement of Cl^- from 1,2-Dichloroethane at the Active Site of *Xanthobacter autotrophicus* Haloalkane Dehalogenase†

Felice C. Lightstone, Ya-Jun Zheng, and Thomas C. Bruice*

Contribution from the Department of Chemistry, University of California, Santa Barbara, California 93106

Received January 14, 1998

Abstract: Molecular dynamics simulations of ground and transition states have been carried out to 540 ps for the S_N2 displacement of Cl^- from 1,2-dichloroethane (DCE) by the Asp124-CO_2^- at the active site of the haloalkane dehalogenase from *Xanthobacter autotrophicus* GJ10. The nucleophilic carboxylate of Asp124-CO_2^- is electrostatically stabilized in the enzyme−substrate (ES) complex by hydrogen bonding. OD1 of Asp124-CO_2^- is hydrogen bonded to water396 and the backbone amide hydrogens of Glu56 and Trp125. The nucleophilic oxygen (OD2) of Asp124-CO_2^- is hydrogen bonded to water323. This is a stable but nonreactive conformation. The kinetically essential near attack conformations (NACs) are formed when water323 dissociates to allow the C(1) of the gauche conformation of DCE to be within ∼3 Å from the nucleophilic OD2 of Asp124-CO_2^- while Cl(1) is hydrogen bonded to the indole NH of Trp125. By comparing the molecular dynamics simulations for the ES complex and the enzyme transition-state (TS) structure, one can observe the changes in the active site structure in the course of the reaction. In contrast to the NAC with a single hydrogen bond between Trp125 and Cl(1), the TS has two hydrogen bonds to the leaving Cl(1), the Trp125 hydrogen bond (2.43 ± 0.29 Å) and the Trp175 hydrogen bond (2.24 ± 0.19 Å). Assistance of the two tryptophan hydrogen bonds to lowering the activation energy may be about 2 kcal/mol. Certain hydrogen bonds are critical to maintaining the tertiary structure of the active site and essential functions of water molecules in the reaction. On comparing the NAC structures to the transition-state structures, hydrogen-bonding changes are seen. These include the already-mentioned electrostatic interaction of Trp175 with Cl(1) in the TS. In the TS, we also observe the formation of a tight hydrogen-bonding matrix involving the water323, water392, and water396. This matrix exactly positions water392 such that it (i) is a member of the triad Asp260-CO_2^-···H−(δ)N−His289−(ϵ)N···water392 and (ii) is aligned correctly to act as a nucleophile toward the carbonyl of the alkyl-ester intermediate (Asp124-CO_2−CH_2CH_2−Cl), formed upon departure of Cl^-. In other words, the ground state of the second enzymatic reaction is set up on reaching the transition state of the first reaction. The hydrogen bond between OD2 of Asp260-CO_2^- and H−(δ)N of His289 exists in both ES and TS structures. Aside from being a part of the catalytic triad for the second reaction, this hydrogen bond is responsible for maintaining the active site structure. Disruption of this hydrogen bond by moving the imidazole proton from H−(δ)N to create H−(ϵ)N of His289 brings about deep-seated changes in the ES ground state such that NACs are not formed. This hydrogen bond is similar to those between Asp and His in the serine esterases where it may also play a role in the stability of the active site.

Introduction

Halogenated organic compounds presently make up one of the largest groups of pollutants. They arise from a variety of sources, including but not limited to herbicides, pesticides, solvents, hydraulic fluids, plasticizers, and chemical intermediates. This fact has spawned an increasing interest in dehalogenation mechanisms, and a concerted effort has been made to use and understand enzymatic dehalogenation for bioremediation purposes. Seven general mechanisms are known for enzymatic dehalogenation: (i) reductive dehalogenation, (ii) oxygenolytic dehalogenation, (iii) hydrolytic dehalogenation, (iv) "thiolytic" dehalogenation, (v) intramolecular substitution, (vi) dehydrohalogenation, and (vii) hydration (Scheme 1).[1] The most well studied hydrolytic aromatic dehalogenase is 4-chlorobenzoyl coenzyme A (CoA) dehalogenase.[2−6] The reaction sequence seems to be well understood (Scheme 2). The haloalkane dehalogenase from the nitrogen-fixing bacterium *Xanthobacter autotrophicus* GJ10 catalyzes the conversion of 1,2-dichloroethane to 2-chloroethanol and chloride without the use of oxygen or cofactors. The reaction sequence for this enzyme involves an S_N2 displacement of chloride by Asp124-CO_2^-, providing a covalently bound ester intermediate (Scheme 3),[7] and in a second step, the ester undergoes hydrolysis to yield 2-chloroethanol as

* To whom correspondence should be addressed. E-mail: tcbruice@bioorganic.ucsb.edu. Fax: (805) 893-2229.

† Abbreviations: DCE, 1,2-dichloroethane; ES, enzyme−substrate; TS, transition state; NAC, near attack conformation; MD, molecular dynamics; rms, root mean square.

(1) Fetzner, S.; Lingens, F. *Microbiol. Rev.* **1994**, *58*, 641.
(2) Zheng, Y.-J.; Bruice, T. C. *J. Am. Chem. Soc.* **1997**, *119*, 3868.
(3) Liu, R.-Q.; Liang, P.-H.; Scholten, J.; Dunaway-Mariano, D. *J. Am. Chem. Soc.* **1995**, *117*, 5003.
(4) Taylor, K. L.; Liu, R.-Q.; Liang, P.-H.; Price, J.; Dunaway-Mariano, D.; Tonge, P. J.; Clarkson, J.; Carey, P. R. *Biochemistry* **1995**, *34*, 13881.
(5) Crooks, G. P.; Xu, L.; Barkley, R. M.; Copley, S. D. *J. Am. Chem. Soc.* **1995**, *117*, 10791.
(6) Taylor, K. L.; Xiang, H.; Liu, R.-Q.; Yang, G.; Dunaway-Mariano, D. *Biochemistry* **1997**, *36*, 1349.

S0002-7863(98)00162-0 CCC: $15.00
Published on Web 05/29/1998

Scheme 1

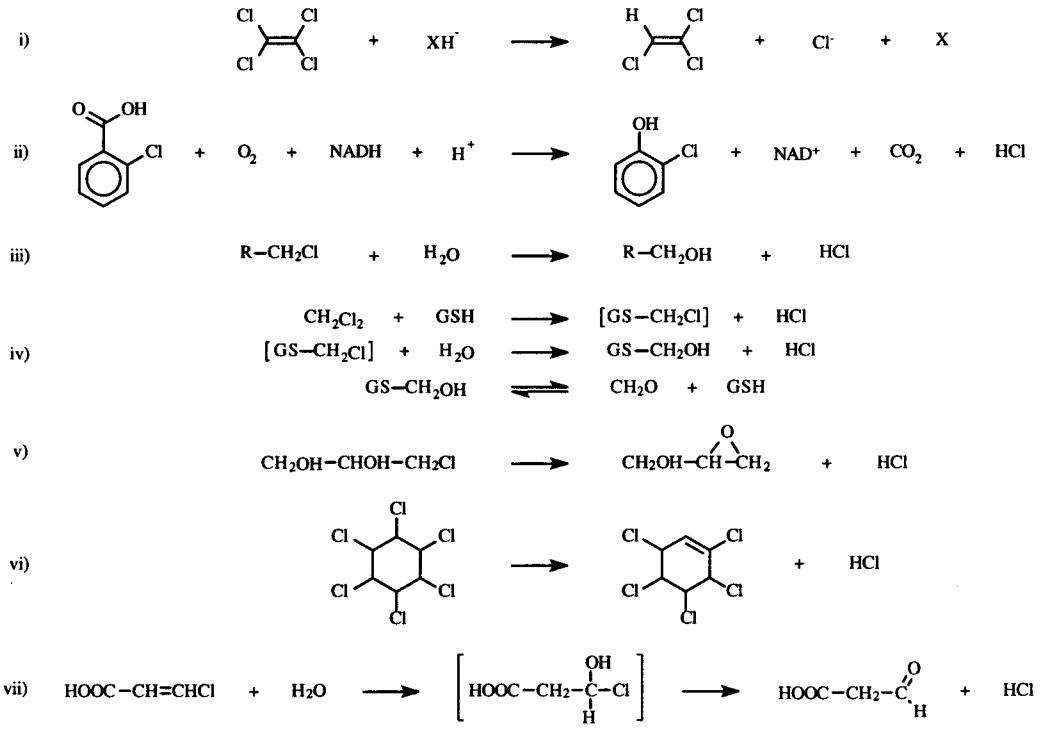

Scheme 2

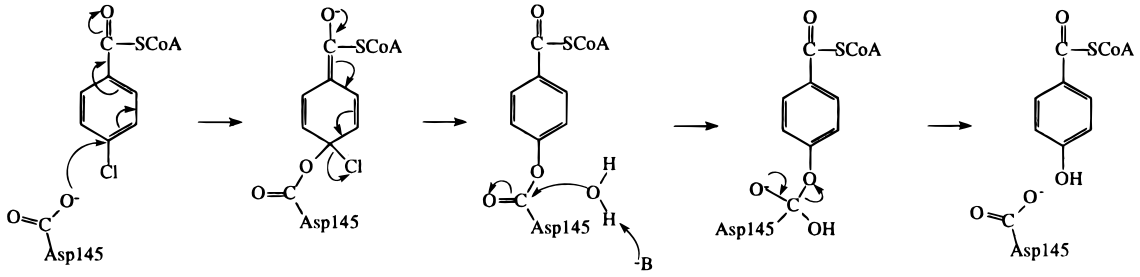

Scheme 3

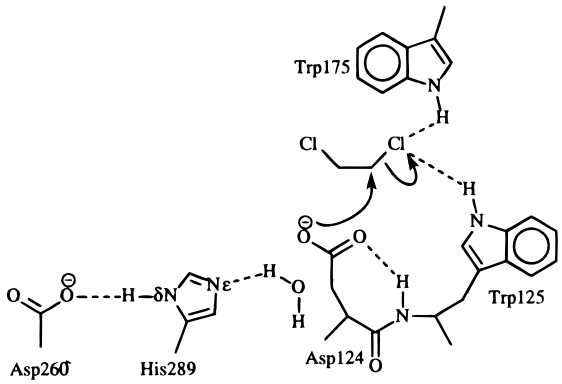

Scheme 4

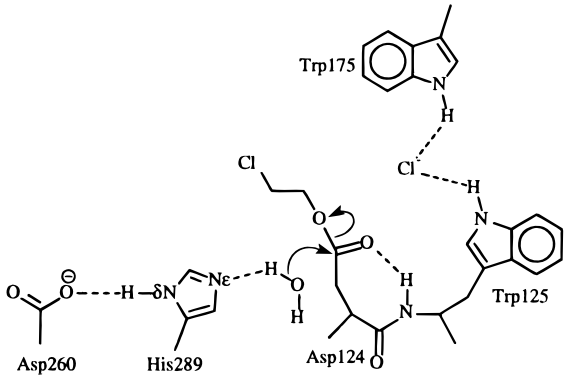

product (Scheme 4). This hydrolysis is believed to involve His289 and Asp260 as a catalytic diad, where His289 is involved in activating a molecule of water which hydrolytically cleaves the ester intermediate (Scheme 4).[8]

This report describes molecular dynamics (MD) simulations of enzyme−substrate (ES) complexes and transition-state (TS) structures associated with the S_N2 displacement of halogen in the first step of catalysis by the *X. autotrophicus* haloalkane dehalogenase (Scheme 3). Our choice of subject is dependent upon the following: (i) existing experimental knowledge concerning S_N2 displacements of anionic leaving groups by anionic nucleophiles and knowing that TS structures for such reactions are comparable in the gas and liquid phase,[9] (ii) S_N2 displacements are associated with only one transition state (no intermediates) such that use of quantum chemical calculations

(7) Verschueren, K. H. G.; Kingma, J.; Rozeboom, H. J.; Kalk, K. H.; Janssen, D. B.; Dijkstra, B. W. *Biochemistry* **1993**, *32*, 9031.

(8) Pries, F.; Kingma, J.; Krooshof, G. H.; Jeronimus-Stratingh, C. M.; Bruins, A. P.; Janssen, D. B. *J. Biol. Chem.* **1995**, *270*, 10405.

(9) Shaik, S. S.; Schlegel, H. B.; Wolfe, S. *Theoretical Aspects of Physical Organic Chemistry. The S_N2 Mechanism*; John Wiley & Sons: New York, 1992.

are simplified, and (iii) a crystallographic structure of *X. autotrophicus* haloalkane dehalogenase is available at 1.9 Å and a structure of this enzyme with 1,2-dichloroethane (DCE) at the active site is available at 2.4 Å (Brookhaven Protein Database: lede and 2dhc, respectively).[10,11]

As a model for the Asp124-CO_2^- attack on DCE, our investigation began with the determination of transition-state structures in the reactions of $CH_3CO_2^-$ (AcO^-) with a number of alkyl halides using ab initio (RHF/6-31+G(d) and HF-SCRF/6+31G(d) levels of theory) and semiempirical (PM3)[12] molecular orbital theory.[13] The ab initio and semiempirical PM3 structures for the TS of the S_N2 displacement of Cl^- from DCE by AcO^-, as judged by the extent of bond formation (O···Cl) and breaking (C···Cl), were quite comparable. Thus, for HF-SCRF/6-31+G(d) and PM3, the ratios of bond breaking, r(C···Cl)/(C−Cl), equal 1.30 and 1.24, respectively, and the ratios of bond making, r(C−O)/(C···O), equal 0.66 and 0.74, respectively. The use of ab initio molecular orbital theory to include the substrate and surrounding enzyme amino acids is not feasible. However, because our semiempirical and ab initio TS structures are quite comparable, we can use PM3 molecular orbital theory for this purpose. In our second study using PM3 semiempirical molecular orbital theory,[14] we examined the reaction coordinate and transition-state structure for the reaction of Asp124-CO_2^- with DCE including the other surrounding 13 amino acids that make up the active site of *X. autotrophicus* haloalkane dehalogenase. We found the transition state in the enzymatic model reaction to be only slightly expanded when compared to the simple reaction of AcO^- with DCE calculated with PM3 molecular orbital theory in the gas phase. Thus, the C···O and the C···Cl distances in the model active site as compared to the gas phase are 1.965 vs 1.942 Å and 2.228 vs 2.196 Å, respectively. In our present report, we use MD simulations to study the entire enzyme as the enzyme−substrate complex and the transition-state structure. Observations have been made which deal with the change of substrate orientation at the active site, the profound dependence of enzyme structure on the protonation state of His289 (ϵN vs δN), and the change in protein conformation and positioning of water molecules in the ground-state attack conformation and the transition state. Of particular concern is the integrity of a hydrogen bond between Asp260-CO2$^-$ and δH of the imidazole of His289 in both catalysis and stabilization of the enzyme structure.

Theoretical Procedure

Molecular dynamics calculations were carried out to 540 ps on Silicon Graphics computers using the AMBER 4.1 programs.[15] Both enzyme−substrate (ES) complex and transition-state (TS) molecular dynamics simulations were run with the N−H proton of the imidazole of His289 on the δN (ES HIδ and TS HIδ) and with the proton on ϵN (ES HIϵ and TS HIϵ). The crystal structure of an ES complex by Verschueren, et al.[11] (Brookhaven Protein Database: 2dhc) was used as the starting structures for the ES HIδ and ES HIϵ simulations. The 1,2-dichloroethane parameters and partial charges used for the ES complex were from Jorgensen et al.,[16] and the parameters for the enzyme were from Cornell et al.[17] Hydrogens were added to the 2dhc crystal structure of the enzyme. The different imidazoles for ϵN- and δN-protonated His289 were requested through the use of Amber by distinguishing them as HID or HIE histidines. In the ES HIδ structure, the δ-proton is hydrogen bonded to Asp260, while with the ES HIϵ structure, the ϵ-proton points away from Asp260 and toward Asp124. The starting structure to generate TS HIϵ was obtained in the following manner. In a previous study,[14] the transition state, along with portions of the enzyme which include the 14 amino acid residues surrounding the substrate, were optimized using PM3. In the PM3 optimization of the transition state and surrounding cavity, the peptide backbone atoms were held fixed to the original X-ray crystallographic coordinates. Thus, it was a simple procedure to overlay the peptide backbones of the PM3-optimized transition state and surrounding amino acids onto the peptide backbones of the crystal structure of the ES complex, remove the overlapped structure, and join in place the PM3 optimized structure carrying the TS. A 50-step steepest decent minimization was performed to provide the starting structure for TS HIϵ simulations in which the His289 ϵ-proton is directed slightly toward Asp260 and the δ-nitrogen points away from Asp260. The TS HIδ structure was taken from the fully composed TS HIϵ enzyme structure. Because His289 was rotated such that the δ-nitrogen was pointed away from Asp260, the His289 side chain was manually rotated 160° such that the proton on the δN could hydrogen bond with a carboxylate oxygen of Asp260. To maintain TS integrity throughout the MD calculations, we assigned large force constants to the transition-state bonds being made and broken and the associated O···C···Cl angle. These parameters are provided in the Supporting Information. The partial charges used for the TS structure were derived from ab initio calculations at the 6-31G-(d) level of theory, using the electrostatic potential at points selected by the CHelpG scheme.[18] In all the simulations, a spherical CAP of waters was requested to be added within 15 Å of the nucleophilic oxygen (OD2) of Asp124-CO_2^- using the EDIT module of AMBER 4.1.[15] However, crystallographic waters seem to have been sufficiently dense since no waters were actually added. Water molecules were treated as TIP3P residues.[19] Once the enzyme structures were completed, 5000 steps of minimization were performed for all four enzyme structures. Molecular dynamics were started with a heating period of 20 ps where the temperature increased from 0 to 300 K and was maintained at 300 K by coupling to a constant-temperature heat bath.[20] The molecular dynamics simulations were continued out another 520 ps with a time step size of 0.002 ps. Nonbonded interactions were cut off at 10 Å and were updated every 25 steps. The SHAKE algorithm[21] was used to constrain all bonds between pairs of atoms. Coordinates were saved for analysis every 100 steps. All plots are shown to 540 ps which includes the heating period. On the basis of the rms fit of the amino acid side chains, the equilibration seems to occur at within 150 ps for the four MD simulations (Figure 1).

(10) Verschueren, K. H. G.; Franken, S. M.; Rozeboom, H. J.; Kalk, K. H.; Dijkstra, B. W. *J. Mol. Biol.* **1993**, *232*, 856.
(11) Verschueren, K. H. G.; Seljée, F.; Rozeboom, H. J.; Kalk, K. H.; Dijkstra, B. W. *Nature* **1993**, *363*, 693.
(12) Stewart, J. J. P. *J. Comput. Chem.* **1989**, *10*, 209.
(13) Maulitz, A. H.; Lightstone, F. C.; Zheng, Y.-J.; Bruice, T. C. *Proc. Natl. Acad. Sci. U.S.A.* **1997**, *94*, 6591.
(14) Lightstone, F. C.; Zheng, Y.-J.; Maulitz, A. H.; Bruice, T. C. *Proc. Natl. Acad. Sci. U.S.A.* **1997**, *94*, 8417.
(15) Pearlman, D. A.; Case, D. A.; Caldwell, J. W.; Ross, W. S.; III, T. E. C.; Ferfuson, D. M.; Seibel, G. L.; Singh, U. C.; Weiner, P. K.; Kollman, P. A. *AMBER 4.1*; University of California, San Francisco, 1995.
(16) Jorgensen, W. L.; McDonald, N. A.; Selmi, M.; Rablen, P. R. *J. Am. Chem. Soc.* **1995**, *117*, 11809.
(17) Cornell, W. D.; Cieplak, P.; Bayly, C. I.; Gould, I. R.; K. M. Merz, J.; Ferguson, D. M.; Spellmeyer, D. C.; Fox, T.; Caldwell, J. W.; Kollman, P. A. *J. Am. Chem. Soc.* **1995**, *117*, 5179.
(18) Breneman, C. M.; Wiberg, K. B. *J. Comput. Chem.* **1990**, *11*, 361.
(19) Jorgensen, W. L.; Chandrasekhar, J.; Madura, J.; Impey, R. W.; Klein, M. L. *J. Chem. Phys.* **1983**, *79*, 926.
(20) Berendsen, H. J. C.; Potsma, J. P. M.; Gunsteren, W. F.v.; DiNola, A. D.; Haak, J. R. *J. Chem. Phys.* **1984**, *81*, 3684.
(21) Gunsteren, W. F. v.; Berendsen, H. J. C. *Mol. Phys.* **1977**, *34*, 1311.

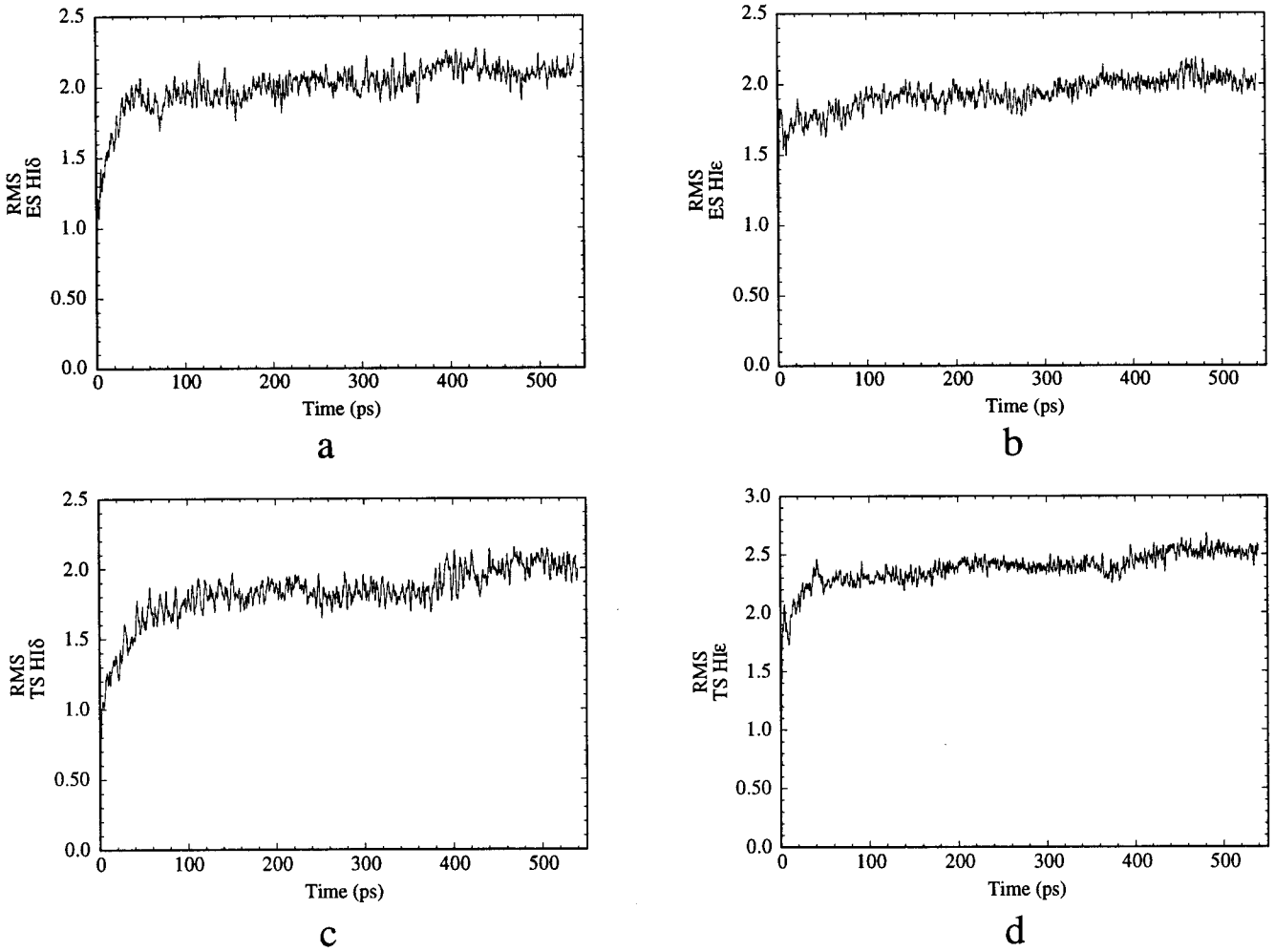

Figure 1. Plots of the rms fit vs time. Each structure in their respective molecular dynamics simulation is compared to the minimized initial structure at time step 0 ps: (a) enzyme−substrate HIδ molecular dynamics simulation; (b) enzyme−substrate HIϵ molecular dynamics simulation; (c) transition-state HIδ molecular dynamics simulation; (d) transition-state HIϵ molecular dynamics simulation. Leveling off of the plots indicate equilibration.

Results and Discussion

The haloalkane dehalogenase has a two-step mechanism for the hydrolysis of a saturated halogenated alkane. To understand the first step of the mechanism (Scheme 3), the ES complex and the TS of the nucleophilic attack of Asp124-CO_2^- on 1,2-dichloroethane (DCE) have now been studied using MD simulations. When studying the ES complex, the interesting ground-state conformations are the ones that allow the reaction to occur. The optimal activity of the haloalkane dehalogenase is at pH 8.2.[10] Assuming that the imidazole group of His289 is subject to the solvent pH, it should not be present as the protonated imidazolium ion. As shown in Scheme 4, His289 is proposed to act as a general base and activate a molecule of water in the second step of the mechanism—the hydrolysis of the alkyl−enzyme ester intermediate.[11] An affect on the ground-state conformations is the position of protonation of the neutral imidazole of His289. In the solution form of histidine, the neutral imidazole proton can be on either the δ or ϵ nitrogen. The pK_a's of the two nitrogens of histidine are very similar, and the equilibrium between the individual tautomeric forms of histidine lies toward protonation of the ϵN.[22,23] However, histidyl residues in proteins have been found to be protonated on the δN.[24] The crystal structures of haloalkane dehalogenase are in accord with the histidine being hydrogen bonded to either Asp260 or Asp124, as shown in Figure 2.[10] This direct evidence only questions, more so, as to which nitrogen of His289 is protonated for the active enzyme. Because His289 is believed to play a functional role in the mechanism, the positioning of the proton on His289 is important. Therefore, MD simulations of the ES complex and the TS were carried out with the proton on the δ- and then on the ϵ-nitrogen of His289 (HIδ or HIϵ). Thus, a total of four dynamics simulations were run: two enzyme−substrate complexes, ES HIδ and ES HIϵ, and two transition-state structures, TS HIδ and TS HIϵ. Including the heating period, all four MD simulations were run for 540 ps.

The enzyme crystal structure contains the substrate at the active site such that direct observation of the substrate orientation is possible (Figure 2).[11] One major point is the conformation of 1,2-dichloroethane (DCE). In the crystal structure, the nonleaving chloro group was assigned to be trans from the leaving chloro group. It should be noted that the electron density of the nonleaving chloro group was weak, and the nonleaving chloro group is determined to be very close to the nucleophilic oxygen (2.97 Å). Certainly, at this distance, the chloro group would feel the repulsion from the negatively charged oxygen of Asp124. Also, the substrate is not oriented for a back-side

(22) Farr-Jones, S.; Wong, W. Y. L.; Gutheil, W. G.; Bachovchin, W. W. *J. Am. Chem. Soc.* **1993**, *115*, 6813.
(23) Görbitz, C. H. *Acta Crystallogr.* **1989**, *B45*, 390.
(24) Fersht, A. *Enzyme Structure and Mechanism*; W. H. Freeman and Co.: San Francisco, CA, 1977.

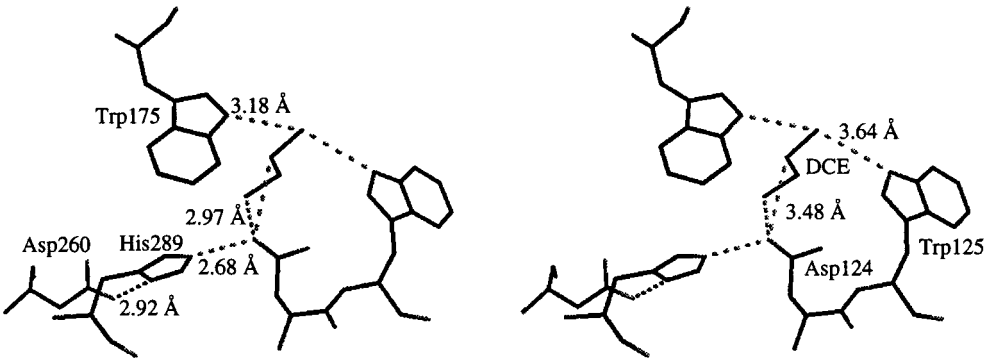

Figure 2. Stereoview of the active site from the X-ray crystal structure.[11] Notice that δN-His289 is only 2.92 Å from OD2 of Asp260 while ϵN-His289 is only 2.68 Å from the nucleophilic oxygen of Asp124. Both distances are short enough to represent hydrogen bonding. Also, notice that DCE is in a trans conformation and the nucleophilic oxygen of Asp124 is only 2.97 Å from the nonleaving chloro group of DCE.

attack by Asp124-CO_2^-. Hence, there seemed to be a need to determine the conformation of the substrate in the active site. From our calculations of the active site model with PM3,[14] the substrate is present in a gauche conformation. Wiberg et al.[25] have investigated the conversion of 1,2-dichloroethane from the trans conformation to the gauche conformation in low-dielectric media, showing the decrease in the gauche−trans free energy difference upon transfer from gas phase to cyclohexane. Jorgensen et al.[16] have shown that their parameters for 1,2-dichloroethane reproduce these findings and should be relevant to hydrophobic regions in proteins. Each of the ES complex molecular simulations will address the conformation of the DCE. Another observation from the crystal structure is the two equidistant hydrogen bonds from Trp125 and Trp175 to the leaving chloro group.[11] This issue will be addressed in each of the four molecular dynamics simulations.

Enzyme−Substrate Complex. The starting structures for the MD studies with both ES HIδ and ES HIϵ were built with a trans conformation for the DCE, as shown in the X-ray coordinates.[11] For the HIδ ES complex, DCE maintains a trans conformation during the energy minimization. However, upon heating to 300 K in the MD studies, the DCE rotates to a gauche conformation at 2.4 ps. For most of the ensuing time of the MD simulation, DCE remains in a gauche conformation. Only during a short period from 417.2 to 423.4 ps does the DCE rotate to a trans conformation (Figure 3). Much the same is true for the HIϵ ES complex where again the dichloroethane stays in a trans conformation during the minimization. But, within 0.4 ps of the heating period, the DCE changes from trans to gauche and remains so for the remainder of the dynamics simulation. Once the dichloroethane orients itself in a gauche conformation, it does not revert to the trans conformation. From our previous PM3 enzyme model calculations and these MD simulations, the substrate must exist in a *gauche* conformation to form productive near-attack conformations.

In previous calculations, the concept of a near-attack conformation has been defined and observed.[26,27] With a historically important series of monophenyl ester intramolecular reactions which mimic the rate enhancements of enzymatic reactions,[28,29] a near attack conformation (NAC) was defined to be an energy minimum structure that geometrically must be formed prior to reaching a transition state in a reaction pathway.[26,27,30] In this intramolecular study, it was shown that the log of the mole fraction of conformations existing as NACs (***P***) was directly proportional to the log of the experimentally determined relative rate constants. Since ***P*** is found to be a function of $\Delta H°$, the driving force of the rate enhancements in these intramolecular reactions is enthalpic rather than entropic. The question arises as to the applicability of these concepts to enzymatic reactions. In reduction reactions involving NAD(P)H as a cofactor, MD simulations show that the planar dihydropyridine moiety is in equilibrium with a unidirectional quasi-boat conformation in which the hydrogen to be transferred as hydride exists in an axial position. Bulky amino acid side chains hinder quasi-boat formation away from the substrate. This anisotropic motion creates productive conformations for the reaction, i.e., NACs.[31−34] The ease of formation of a NAC determines the number of NACs formed in a period of time and, thus, the likelihood of reaction. This is also consistent with the fact that close proximity of the electrophile and the nucleophile increases the rate of reaction.[28,29] To apply these concepts to the haloalkane dehalogenase, we were interested in seeing if NAC formation occurs during the MD simulations of

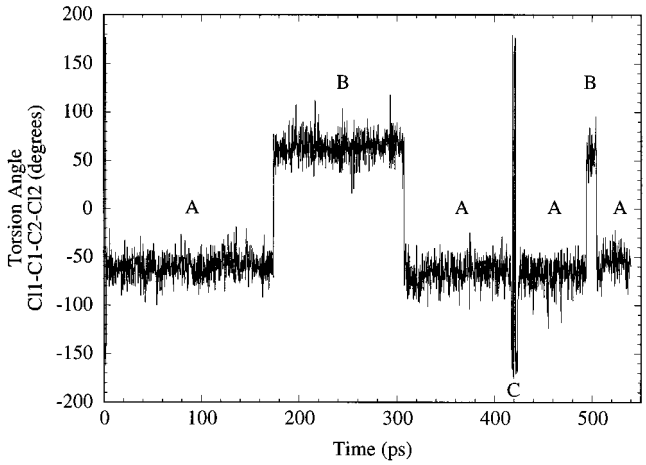

Figure 3. Plot of the torsion angle (Cl−C−C−Cl) of 1,2-dichloroethane (DCE) vs time for the enzyme−substrate HIδ molecular dynamics simulation. DCE is in a gauche conformation when at $-62.3° \pm 12.9°$ (position A) and $64.7° \pm 12.6°$ (position B). DCE is in a trans conformation when at $\pm 180°$ (position C).

(25) Wiberg, K. B.; Keith, T. A.; Frisch, M. J.; Murcko, M. *J. Phys. Chem.* **1995**, *99*, 9072.
(26) Lightstone, F. C.; Bruice, T. C. *J. Am. Chem. Soc.* **1996**, *118*, 2595.
(27) Lightstone, F. C.; Bruice, T. C. *J. Am. Chem. Soc.* **1997**, *119*, 9103.
(28) Bruice, T. C.; Pandit, U.K. *Proc. Natl. Acad. Sci. U.S.A.* **1960**, *46*, 402.
(29) Bruice, T. C.; Pandit, U.K. *J. Am. Chem. Soc.* **1960**, *82*, 5858.
(30) Lightstone, F. C.; Bruice, T. C. *J. Am. Chem. Soc.* **1994**, *116*, 10789.
(31) Almarsson, Ö.; Karaman, R.; Bruice, T. C. *J. Am. Chem. Soc.* **1992**, *114*, 8702.
(32) Almarsson, Ö.; Bruice, T. C. *J. Am. Chem. Soc.* **1993**, *115*, 2125.
(33) Almarsson, Ö.; Sinha, A.; Gopinath, E.; Bruice, T. C. *J. Am. Chem. Soc.* **1993**, *115*, 7093.
(34) Luo, J.; Bruice, T. C. To be published, 1998.

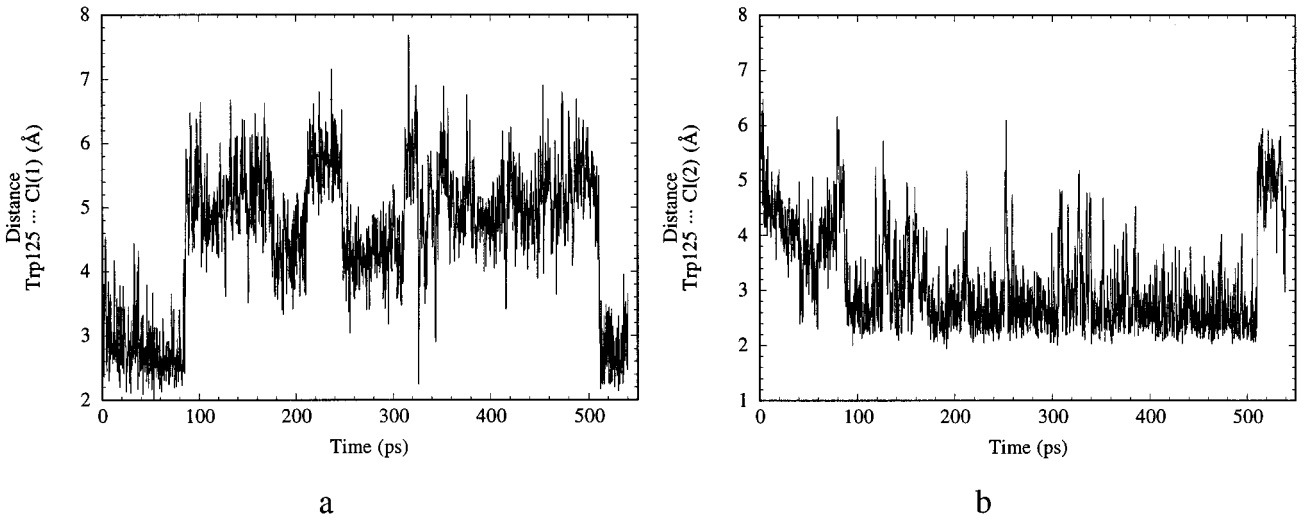

Figure 4. Indole nitrogen of Trp125 is observed to be hydrogen bonded to either Cl(1) or Cl(2) of 1,2-dichloroethane in the enzyme−substrate HIδ molecular dynamics simulation. (a) Plot of the distance between the indole nitrogen of Trp125 and the departing Cl(1) vs time. Hydrogen bonding is observed from 0 to ∼85 ps and from ∼511 to 540 ps. (b) Plot of the distance between the indole nitrogen of Trp125 and Cl(2) vs time. Hydrogen bonding is observed from approximately 87 to 510 ps.

the ES complexes and in which simulation (ES HIδ vs ES HIϵ) they occur the most often. We will first consider the MD for the ES HIδ complex since these results are descriptive of what the ground state must closely resemble.

For the ES HIδ Simulation, equilibration of the MD occurs approximately at 100 ps. Trp125 plays a critical role in properly aligning the DCE for reaction with Asp124. A hydrogen bond between the chloro substituent of a chloroalkane and an indole N−H function must seem rather feeble, but in the hydrophobic pocket of the active site (Trp125, Phe128, Phe172, Trp175, Leu179, Val219, Phe222, Val226, Leu262, Leu263, and His289), the electrostatic forces are sufficient. During the entire dynamics simulation, Trp125 is hydrogen bonded to either Cl(1) or Cl(2) of the substrate (Figure 4). This hydrogen bonding assists in guiding the substrate to the edge of the hydrophobic core to the vicinity of Asp124. Trp175 is never observed to hydrogen bond to the substrate. The non-nucleophilic carboxylate oxygen (OD1) of Asp124-CO_2^- is hydrogen bonded to two amide hydrogens throughout the MD, one of Glu56 and one of Trp125. During the heating period, water396 moves to hydrogen bond to the nucleophilic oxygen (OD2) of Asp124-CO_2^- (0.8 ps) and then moves to hydrogen bond to OD1 of Asp124-CO_2^- (4 ps). All through the MD simulation, a strong hydrogen bond is observed between the OD2 of Asp260-CO_2^- and H-δN of His289. Only briefly during equilibration (60 to 90 ps) does this hydrogen bond become interrupted by water433 becoming the hydrogen bond partner, replacing His289. At this time, the following cascade of events occur. Water323 remains hydrogen bonded to ϵN-His289 while the imidazole ring of His289 rotates from approximately 110° to approximately 200°. The hydrogen bond between water323 and the peptidic carbonyl of Glu56 is disrupted. By ∼85 ps, water323 has migrated to hydrogen bond with Asp124-CO_2^- which is the nearest charged group. At this point, equilibration of the MD simulation nears completion and water323 bridges the nucleophilic oxygen OD2 of Asp124-CO_2^- and the indole NH of Trp175 by hydrogen bonding to both.

The non-nucleophilic oxygen (OD1) of Asp124-CO_2^- is hydrogen bonded to water396 and two backbone amide hydrogens, Glu56 and Trp125. These four hydrogen bonds to Asp124-CO_2^- provide electrostatic stabilization to the carboxylate anion. However, approach of the nucleophilic OD2 to C(1)

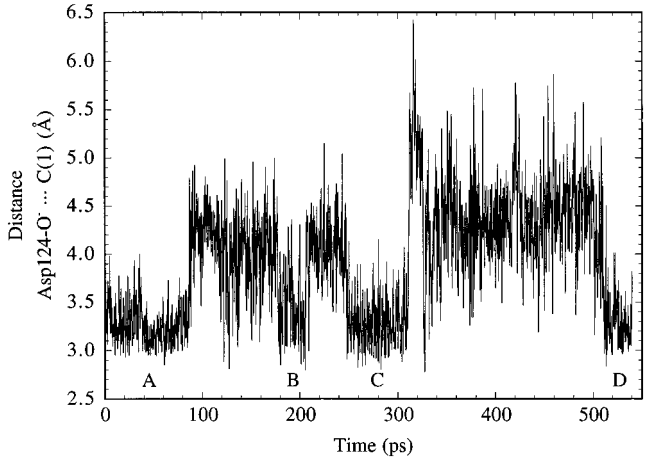

Figure 5. Plot of the distance between the nucleophilic oxygen OD2 of Asp124-CO_2^- and C(1) of 1,2-dichloroethane (DCE) vs time for the enzyme−substrate HIδ molecular dynamics simulation. Notice that positions marked by A, B, C, and D are when the OD2 of Asp124-CO_2^- is within attacking distance of C(1) of DCE. However, NACs should also have hydrogen bonds between the indole nitrogen of Trp125 and the departing chloro substituent. NACs are formed from ∼511 to 540 ps (position D).

of DCE is sterically prohibited by water323. To form a NAC, water323 must dissociate from Asp124-CO_2^-. From 510 ps to completion of MD at 540 ps, water323 drifts away from Asp124-CO_2^- and NACs are formed, as shown in Figure 5. The C(1) of DCE approaches the OD2 of Asp124-CO_2^- to distances of ∼3.00 Å. Also, this motion places electrophilic C(1) of DCE in line for an S_N2 reaction with OD2. The NAC maintains the hydrogen bond between the indole H-N of Trp125 and Cl(1) of DCE (Figure 6).

In the MD Simulation of the ES HIϵ Complex, essentially no NACs were observed in which Asp124-CO_2^- would be positioned for an S_N2 displacement of Cl^- from DCE. Both directly and indirectly, having the proton on the ϵN of His289 changes the active site structure drastically. Similar to the ES HIδ simulation, equilibration occurs approximately at 120 ps. After minimization of the structure, His289 is hydrogen bonded to the carboxylate of Asp124 and remains so for the first 190 ps of MD (Figure 7). This hydrogen bond would, of course,

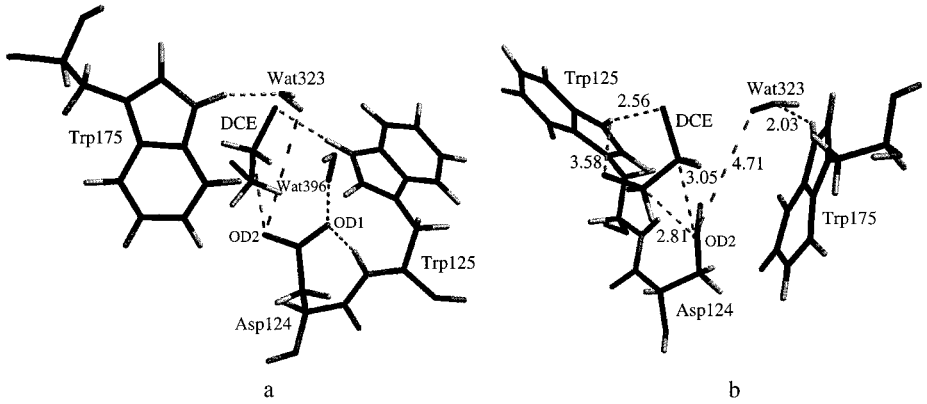

Figure 6. (a) Snapshot of the active site in a NAC during the enzyme−substrate HIδ molecular dynamics simulations. (b) An orthogonal view of a. Notice that water323 is dissociated from Asp124 (4.71 Å). DCE is within attacking distance by the OD2 of Asp124-CO_2^- (3.05 Å), and Cl(1) is hydrogen bonded to the indole of Trp125 (2.56 Å). All distances are shown in angstroms.

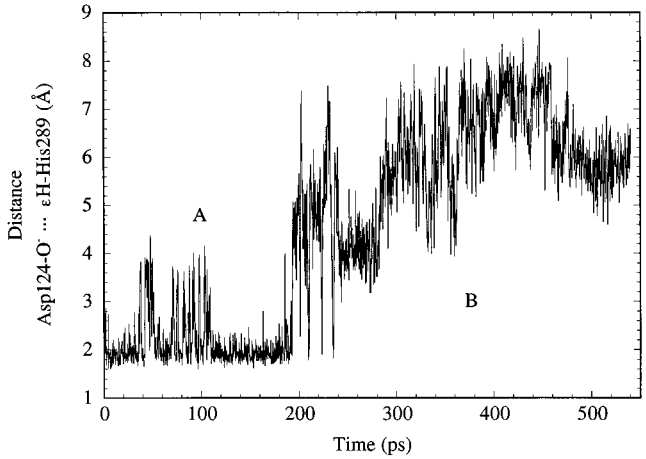

Figure 7. Plot of the distance between the OD2 of Asp124-CO_2^- and ϵH of His289 vs time for the enzyme−substrate HIϵ molecular dynamics simulation. From 0 to 193 ps, Asp124-CO_2^- is mostly hydrogen bonded to ϵH-His289 and pointed into the active site (position A). From 193 to 540 ps, Asp124-CO_2^- is rotated away from the active site (position B).

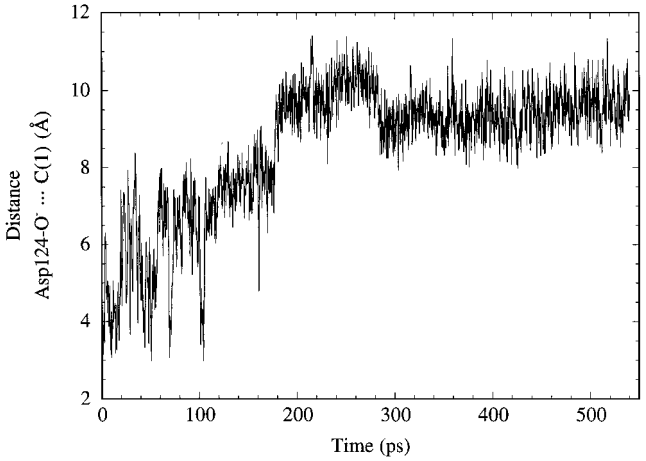

Figure 8. Plot of the distance between the OD2 of Asp124-CO_2^- and the electrophilic carbon of DCE vs time for the enzyme−substrate HIϵ molecular dynamics simulation. Notice that DCE drifts away from Asp124. By 300 ps, DCE is approximately 9 Å away from Asp124.

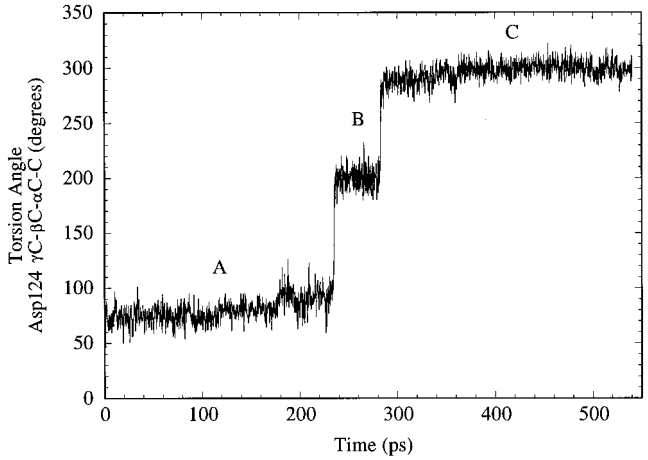

Figure 9. Plot of the torsion angle (γC−βC−αC−C) of Asp124 vs time for the enzyme−substrate HIϵ molecular dynamics simulation. Asp124 starts with its carboxylate group pointed into the active site at 79.9° ± 10.9° (position A). At ∼235 ps, the carboxylate group turns slightly away from the active site at 198.4° ± 13.09° (position B). Finally, at ∼283 ps, the carboxylate group is completely turned away from the active site at 296.6 ° ± 8.3 ° (position C).

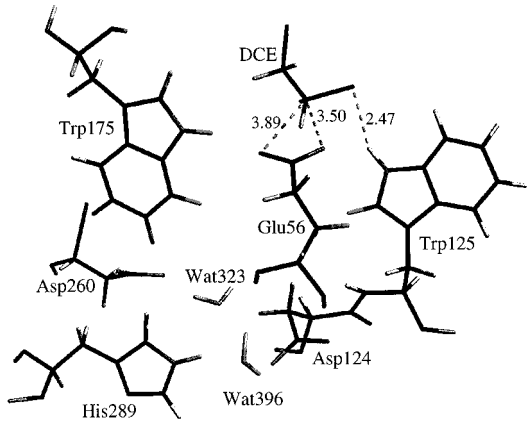

Figure 10. Snapshot of the disrupted active site from the enzyme−substrate HIϵ molecular dynamics simulation. Notice that Glu56 is turned into the active site while Asp124 is turned away from the active site. The indole nitrogen of Trp125 is hydrogen bonded to Cl(1) of 1,2-dichloroethane. All distances are shown in angstroms.

decrease the nucleophilicity of the attacking carboxylate oxygen and seemingly disrupts the integrity of the active site. Examination of Figure 8 shows that, as the MD simulation starts, the OD2 of Asp124-CO_2^- is located 3.34 Å from the DCE carbon C(1) which undergoes nucleophilic attack in the enzymatic reaction. With time, the substrate drifts away, and between 300 and 540 ps, the OD2 of Asp124-CO_2^- is approximately 9 Å away from both carbons of DCE, such that no reaction can occur

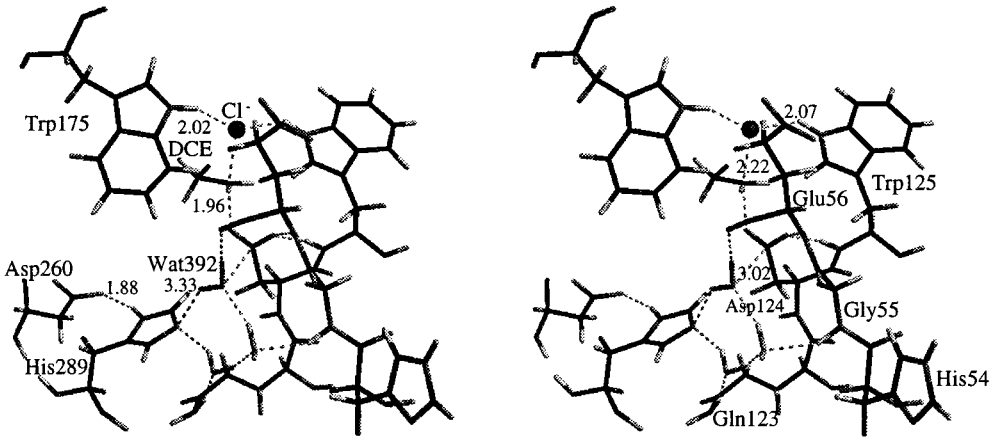

Figure 11. Stereoview of a snapshot of the active site from the transition-state HIδ MD simulation. Notice that the indole nitrogens of Trp125 and Trp175 are hydrogen bonded to the departing chloride from DCE (2.02 Å and 2.07 Å, respectively). His289 is hydrogen bonded to Asp260 (1.88 Å). The hydrogen-bonding matrix is shown in the forefront. Water392 is shown between His289 and Asp124. Water392 is within attacking distance of γC-Asp124.

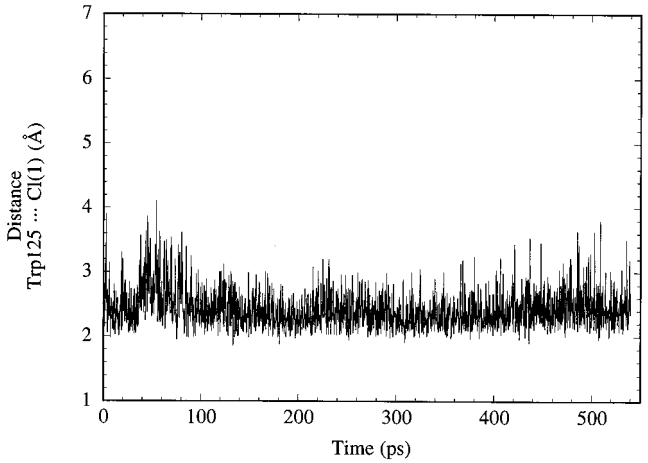

Figure 12. Plot of the distance between the indole nitrogen of Trp125 and the departing chloride from DCE vs time for the TS HIδ MD simulation. Trp125 is constantly hydrogen bonded to the substrate, DCE.

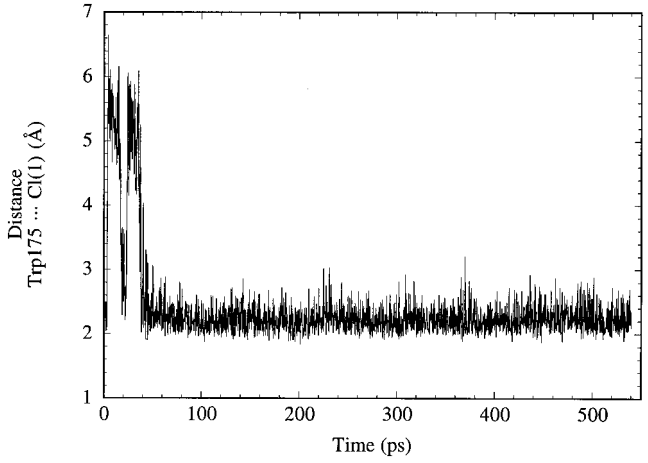

Figure 13. Plot of the distance between the indole nitrogen of Trp175 and the departing chloride vs time for the TS HIδ MD simulation. After equilibration, Trp175 is constantly hydrogen bonded to the substrate Cl(1) in the TS.

(Figure 8). Subsequently, the hydrogen bond between Asp124 and His289 is broken, and the Asp124 side chain is observed to rotate out of the active site (Figure 9). The first rotation is 130° from its original orientation (as observed by the torsion angle defined by γC−βC−αC−C), and then the second rotation is 230° from its original orientation. These consecutive rotations allows the carboxylate group of Asp124-CO_2^- to hydrogen bond to the amide group of Gln123 and directs the carboxylate group to the other side of the peptide backbone, taking it out of the active site (Figure 10).

Trp125 is hydrogen bonded to Cl(1) of dichloroethane. However, this bond does not persist throughout the course of the simulation. Similar to the ES HIδ MD, Trp175 never hydrogen bonds to the substrate. There are only two snapshots at 104.2 and 104.4 ps (before completion of equilibration) where Asp124 is within attacking distance (3.03 and 3.04 Å) to C(1) of DCE and where Trp125 has a hydrogen bond to the chlorine on C(1) (2.81 and 2.51 Å). This happens when His289 is at non-hydrogen-bonding distances of 3.46 and 3.81 Å from Asp124.

The most detrimental change in the conformation of the active site of the ES HIϵ complex is that the carboxyl group of Glu56 turns into the active site. The starting (X-ray) structure has the carboxyl group of Glu56 facing away from the active site, such that Asp124-CO_2^- is the only negatively charged group in the active site. Within 2 ps of the heating period of the MD simulation, Glu56 turns into the active site. Throughout the remainder of the dynamics simulation involving ES HIϵ, Glu56 is completely stable with the carboxylate group remaining in the active site. With Asp124 hydrogen bonded to His289, and the new Glu56 carboxylate group in the active site, the substrate becomes attracted to Glu56 and moves toward it (Figure 10). A possible explanation available is that the ϵH of His289 is hydrogen bonded to Asp124, changing the conformation of the enzyme to allow Glu56 to orient itself into the active site. Alternatively, an alteration in the active site could hinge on the lack of a hydrogen bond between His289 and Asp260, the proposed catalytic diad. In point mutation studies where Asp260 is changed to Asn, the enzyme is completely inactive.[35] More importantly, Krooshof et al. find the mutant to be highly unstable. However, by creating a double point mutation where Asp260 is changed to Asn and Asn148 is changed to Asp, this mutant has a 220-fold decrease in activity from the wild type. Here, the double mutant has a hydrogen bond between Asp148 and His289, such that His289 is in a relatively similar position as the wild type. Clearly, the position of His289 is essential to the structure and stability of the enzyme, where His289 is preferably hydrogen bonded to Asp260.

(35) Krooshof, G. H.; Kwant, E. M.; Damborský, J.; Koca, J.; Janssen, D. B. *Biochemistry* **1997**, *36*, 9571.

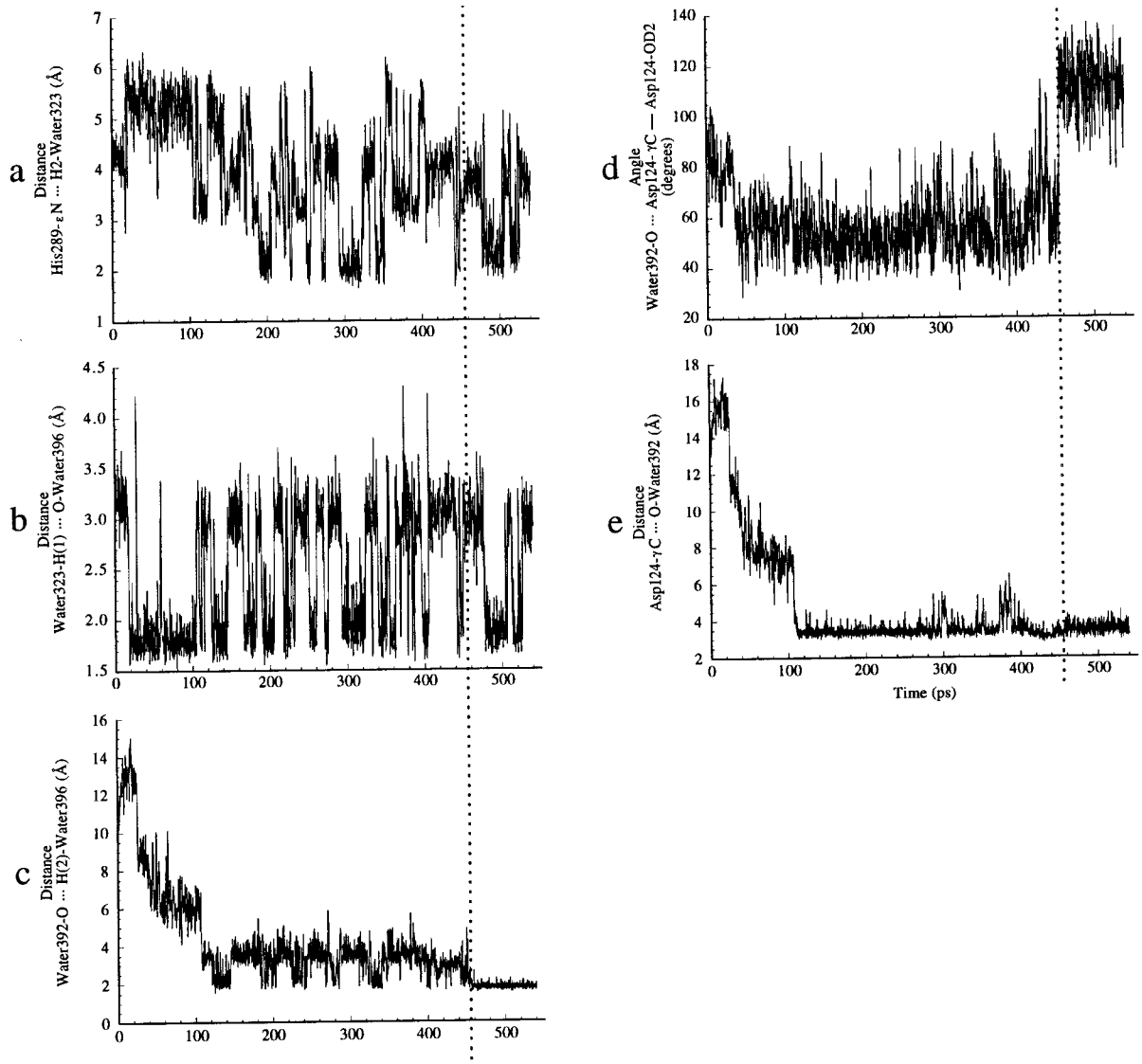

Figure 14. Plots that describe the formation of the catalytic triad and the hydrogen-bonding matrix over time for the TS HIδ molecular dynamics simulation. (a) Plot of the distance between ϵN of His289 and a hydrogen of water323 vs time. (b) Plot of the distance between a hydrogen of water323 and the oxygen of water396 vs time. (c) Plot of the distance between the oxygen of water392 and a hydrogen of water396 vs time. (d) Plot of the angle of nucleophilic attack by water392 on Asp124 as defined by water392-O, Asp124-γC, and Asp124-O vs time. (e) Plot of the distance between the nucleophilic oxygen of water392 and the γC of Asp124 vs time. Considering a and b together, one hydrogen of water323 is hydrogen bonded to water396 (under 2 Å) while water323 moves to hydrogen bond to His289 ~185 ps (~2.2 Å). Considering c, d, and e together, water392 moves toward water396 (c) and Asp124 (e). Though water392 is close to Asp124 and is occasionally hydrogen bonded to water396, it is not until ~456 ps that water392 is in the proper angle (112.2 ± 9.9°) for nucleophilic attack on the electrophilic γC-Asp124 (d). At this time the hydrogen bond between water392 and water396 becomes extremely tight and stable (c).

From the foregoing discussion, the choice of positioning the proton on either the δN or the ϵN of His289 produces drastically different simulations. The ES simulation with the proton on the δN of His289 (HIδ) provides a structure consistent with experimental data. A hydrogen bond is observed between Asp260 and His289, and Trp125 is constantly hydrogen bonded to either chloro group of dichloroethane. Most importantly, productive NACs are able to form, allowing a reaction to take place. From these dynamics simulations, the only limiting factor for the S_N2 displacement of chloride by aspartic acid seems to be precise substrate orientation, i.e., NAC formation. The ES simulation with the ϵN protonated (HIϵ) results in a disrupted active site and essentially no productive conformations for reaction.

Transition-State Structure. An enzyme must be able to change shape to accommodate the transition states and intermediate-state structures. From an earlier study, the coordinates of 14 amino acids, Glu56, Asp124, Trp125, Phe128, Phe172, Trp175, Leu179, Val219, Phe222, Pro223, Val226, Leu262, Leu263, and His289, which make up the active site for the S_N2 displacement of Cl^-, as well as the substrate DCE, were taken from the enzyme−substrate crystal structure[11] and were optimized along with the transition state of the S_N2 displacement of Cl^-.[14] This optimized transition-state structure in the active site has now been reconstituted into the whole enzyme structure for MD simulations. To maintain this transition-state structure throughout the MD simulations, the making and breaking bonds in the TS, as well as the angle between the attacking and leaving group, were held fixed by large force constants. In this manner, the enzyme was free to adapt to the structural needs of the transition state. Structural changes in the protein in order to reach the transition state are our primary concern. Two sets of dynamics simulations were carried out to 540 ps, one with the proton on the δN of the imidazole of His289 (TS HIδ) and the

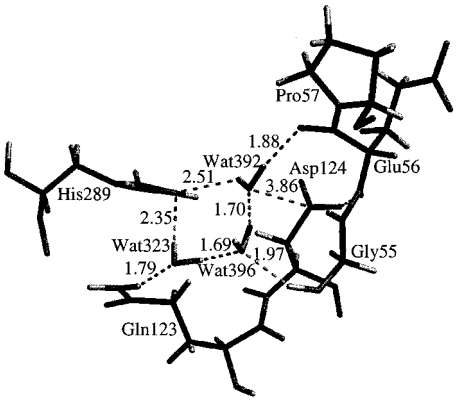

Figure 15. Snapshot of the hydrogen-bonding matrix formed during the transition-state HIδ MD simulation. Water392 becomes the nucleophilic water molecule for the ester hydrolysis and is located on the axis between Asp124 and His289. The TS for DCE is not shown. All distances are shown in angstroms.

other with the proton on the ϵN (TS HIϵ). Analogous to the ES MD simulations where ES HIδ provides a sensible ground state and ES HIϵ does not, TS HIδ provides a satisfying enzyme transition state, whereas TS HIϵ does not. We will consider TS HIδ first.

In the TS HIδ Simulation, both Trp125 and Trp175 are hydrogen bonded to departing Cl(1) of DCE, as shown in Figure 11. Trp125 starts hydrogen bonded to Cl(1) of the TS and stays hydrogen bonded at an average distance of 2.43 $\pm$ 0.29 Å (Figure 12). The simulation starts with Trp175 hydrogen bonded to Cl(1) of the TS. However, during heating and equilibration (from 3.2 to 19 ps and from 23.4 to 38 ps, as shown in Figure 13), Trp175 temporarily loses this hydrogen bond. After 38 ps, Trp175 is continually hydrogen bonded to Cl(1) at an average distance of 2.24 $\pm$ 0.19 Å. Comparing these hydrogen-bonding distances with the respective calculated PM3 transition-state distances, the general perception is that the hydrogen bond formed between Trp175 and Cl(1) of the TS is tighter than the like hydrogen bond formed with Trp125. However, given the standard deviation for the hydrogen bonds in the MD run, the chloride is essentially equidistant from the two tryptophans.

In the X-ray structure of the alkyl−enzyme ester intermediate,[11] Asp260-CO_2^- is in position to allow hydrogen bonding to the δN−H of the imidazole of His289 which in turn is in position to hydrogen bond to a water molecule (Scheme 4). This hydrogen-bonded water molecule is at an improper angle and distance to attack the ester carbonyl carbon. In our MD simulations, a catalytically significant change in the positions of water323, water392, and water396 is seen on comparing the simulated MD structure of the ES complex to the MD simulated structure of the enzyme TS for the S_N2 displacement of Cl^-. The formation of the triad consisting of Asp260, His289, and water392 for hydrolysis of the alkyl−enzyme ester intermediate is seen to be present in the TS simulation. Thus, the triad geometry is formed while E·S goes to E·TS. This triad resembles that seen in the serine esterases. A very constant hydrogen bond exists between Asp260 and His289 (2.82 $\pm$ 0.12 Å). Water392 starts ~13.7 Å away from Asp124, approaches Asp124, and becomes the nucleophilic water for the second step of the mechanism (Figure 14e). This transformation takes place during formation of the TS of the first step. Details follow.

From 25.6 to 107 ps, water392 approaches His289 and is hydrogen bonded to other waters. After 107 ps, Trp175 and His289 move slightly away from each other allowing water392 to squeeze by and approach Asp124 (Figure 14e). The state of affairs between 108 and 453 ps is (i) water392 and the carboxylate of Asp124-CO_2^- are on average 3.53 $\pm$ 0.47 Å apart, but water392 is not at a suitable angle for nucleophilic attack on γC of Asp124 for the second step of the reaction (Scheme 4), (ii) water323 is orienting itself with water396 and His289—the orientations include H(2) of water323 hydrogen bonded to His289, and H(1) is usually hydrogen bonded to water396 (Figure 14a and 14b), and (iii) on occasion H(1) of water323 hydrogen bonds to His289. After 453 ps, a hydrogen-bonding network of all three waters is formed (water 323, water 396, and water392) in a cluster with His289, Gly55, and Gln123 (Figures 14 and 15). It is at this time that water392 is positioned to attack the carbonyl of Asp124-$CO_2CH_2CH_2Cl$ upon ester formation from the TS. As shown in Figure 14d, this is clearly evident because water392 moves to an appropriate angle (112.2 $\pm$ 9.9°) for nucleophilic attack on the ester carbonyl which is being formed from the TS. Water392 stays in this orientation from 455.8 ps to the end of the simulation. Here, we observe the catalytic apparatus for the second step of the catalytic process to be present in the enzyme TS structure but not in the structure

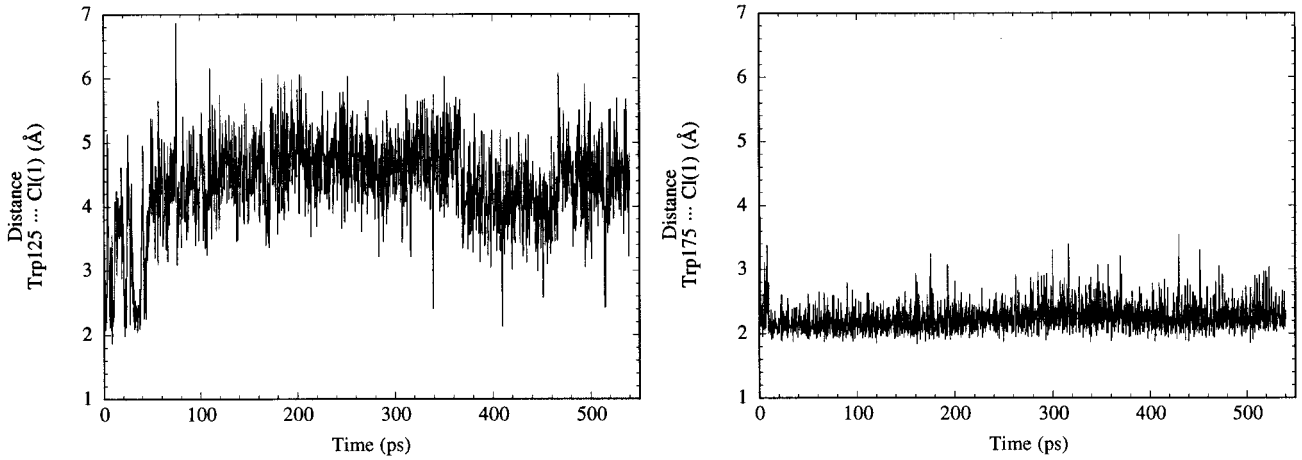

Figure 16. (a) Plot of the distance between the indole nitrogen of Trp125 and the departing chloride of DCE vs time for the TS HIϵ MD simulation. (b) Plot of the distance between indole nitrogen of Trp175 and the departing chloride of DCE vs time for the TS HIϵ MD simulation. Notice that Trp125 never forms a hydrogen bond with the departing chloride of DCE, while Trp175 is constantly hydrogen bonded to the departing chloride of DCE.

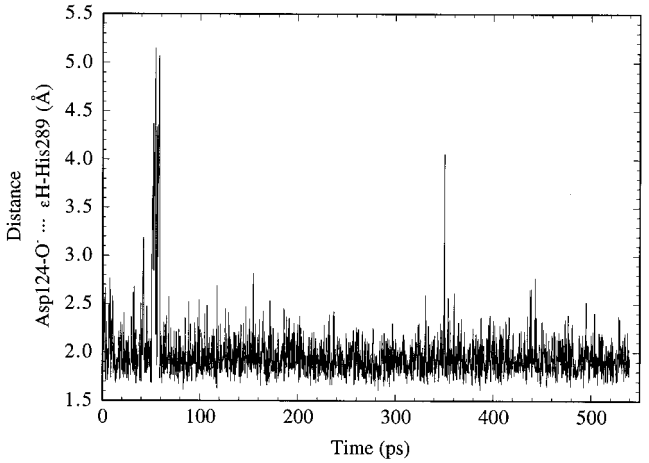

Figure 17. Plot of the distance between the OD2 of Asp124-CO_2^- and ϵH of His289 vs time for the TS HIϵ MD simulation. Notice that there is a strong and constant hydrogen bond between the OD2 of Asp124-CO^{2-} and ϵH of His289 after equilibration (1.94 ± 0.17 Å).

of the ES NAC. It seems most reasonable to suppose that the catalytic apparatus for the second step is formed along with the TS that then yields the substrate for the second step.

For the TS HIϵ Simulation, Trp125 is never observed to hydrogen bond to departing Cl(1) of DCE (Figure 16a), while Trp175 is continuously hydrogen bonded to Cl(1) (Figure 16b). The ES HIϵ MD simulations essentially never provide the productive features of a NAC. However, if we assume that the ES HIϵ could result in a TS, it is unlikely that Trp125 orients the DCE (ES HIϵ), and then only Trp175 assists the chloride to leave (TS HIϵ). As observed in the ES HIϵ dynamics simulation, the hydrogen bond between His289 and the nucleophilic oxygen of Asp124 remains in the transition state (Figure 17). Obviously, a TS bearing the imidazole of His289 hydrogen bonded to the entering OD2 of Asp124-CO_2^- is not acceptable. In addition, the catalytic diad between Asp260 and His289 never forms.

Conclusion

By combining the information from all four dynamics simulations, we show that the proton of the neutral imidazole of His289, in both ground and transition states, is located on δN. In the active site of haloalkane dehalogenase, DCE is no longer solvated by water but is surrounded by a hydrophobic milieu created by the aliphatic $-CH_2CH_2-$ moiety of Glu56; the aliphatic side chains of Leu179, Leu262, Leu263, Val219, and Val226; the aromatic side chains of Trp125, Trp175, Phe128, Phe172, and Phe222; and the heterocyclic ring of Pro223. Electrostatic interaction of indole NH of Trp125 with the Cl(1) and Cl(2) substituents maintains DCE in the vicinity of the nucleophilic Asp124-CO_2^- located at the edge of the hydrocarbon milieu. The OD2 of Asp124-CO_2^- carries out an S_N2 displacement of Cl^- from DCE to provide the intermediate Asp124-$CO_2-CH_2CH_2-$Cl. S_N2 displacements involving anionic nucleophiles and leaving groups are about 10^{16} faster in the gas phase than in water[36] because desolvation of the nucleophile and solvent reorganization upon forming the transition state is unnecessary. The low dielectric hydrocarbon cavity which surrounds the substrate provides the advantage and also the pronounced expression of electrostatic effects. Moreover, the bringing together of reactants in a NAC and this low dielectric must be the main driving forces for the enzymatic reaction, as compared to the reaction in water. Secondary is the electrostatic assistance to the departure of Cl^- by equidistant hydrogen bonding of Cl(1) to Trp125 and Trp175 in the TS. The mutagenesis studies of Kennes et al. established the importance of Trp125 and Trp175 in catalysis.[37] The hydrogen bond to Trp175 does not exist in the ground state such that it's presence in the TS provides for additional electrostatic stabilization. It has been determined by mutation experiments that exchange of Trp125 by Phe decreases k_{cat}/K_m by 20-fold (~1 kcal/mol).[37] The equidistant hydrogen bonds from Trp125 and Trp175 are probably worth but ~2 kcal/mol in decreasing the activation energy by assisting Cl^- departure. An additional role of the tryptophans is to hold the chloride ion during the subsequent hydrolysis of the intermediate ester Asp124-$CO_2-CH_2CH_2-$Cl (Scheme 4).[7]

The carboxylate moiety of the Asp124-CO_2^- is stabilized by hydrogen bonding to water323, water396, and the backbone amide hydrogens of Glu56 and Trp125. Water323 is in an equilibrium between hydrogen bonding to OD2 of Asp124-CO_2^- and not being so. When water323 moves away from OD2, the C(1) of DCE moves to ~3 Å distance of OD2 for an S_N2 displacement of Cl^-. NACs with this characteristic prevail in the last 30 ps of MD simulation. A feature of the active site is that the waters which stabilize Asp124 in the ES complex are part of the structure of the NAC for the second step of the mechanism.

As the transition state for the S_N2 reaction is formed, there is also formed a triad of Asp260-CO_2^- hydrogen bonded to the H-δN of His289 which is hydrogen bonded to water392. The Asp260-$CO_2^-\cdots$H$-(\delta)$N$-$His289$-(\epsilon)$N$\cdots$water392 catalytic triad provides for general-base catalysis of water392 attack on the carbonyl of the eventual ester intermediate. It has been previously shown that changing His289 to Gln by mutagenesis does not result in the abolishment of the S_N2 displacement of chloride by Asp124[8] but does result in the accumulation of the Asp124-$CO_2-CH_2CH_2-$Cl intermediate. Of considerable interest is that the triad required in the ground state of the enzyme for hydrolysis of the Asp-$CO_2-CH_2CH_2-$Cl intermediate (second step of the mechanism) is created simultaneously with formation of the TS which leads to ester intermediate formation (first step of the mechanism).

Acknowledgment. This work was supported by grants from the NIH and the Petroleum Research Fund of the American Chemical Society. This work was also partially supported by the National Center for Supercomputing Applications, University of Illinois at Urbana-Champaign, under CHE970032N.

Supporting Information Available: Tables of bond, angle, and torsional parameters and atomic charges (3 pages, print/PDF). See any current masthead page for ordering information and Web access instructions.

JA980162J

(36) Nibbering, N. M. M. In *Advances in Physical Organic Chemistry*; Bethell, D., Ed.; Academic Press: San Diego, CA, 1988; Vol. 24, p 1.

(37) Kennes, C.; Pries, F.; Krooshof, G. H.; Bokma, E.; Kingma, J.; Janssen, D. B. *Eur. J. Biochem.* **1995**, *228*, 403.